An X-ray Test Facility for Diffraction Gratings

Randall L. McEntaffer*[a], Fred R. Hearty[a], Brian Gleeson[a], Webster Cash[a]
[a]University of Colorado, Center for Astrophysics and Space Astronomy, 593 UCB,
1255 38th St., Boulder, CO 80309-0593

Abstract

The University of Colorado maintains a grating evaluation facility to characterize optics from the far ultraviolet to the X-ray. The newest addition to this facility is a novel X-ray monochromator. Light is generated by a Manson electron impact X-ray source and passes through a monochromator which incorporates a grating in the off-plane mount at grazing incidence followed by an aluminum filter. From here, the light enters another vacuum chamber to illuminate the test grating, which disperses light onto a resistive anode MCP. This monochromator is characterized utilizing a variety of source anodes and voltages. Preliminary results from a high density test grating, also in the off-plane mount, display that this system is a highly effective tool for determining grating efficiencies.

1. Introduction

1.1 Off-plane geometry

The off-plane mount at grazing incidence brings light onto the grating at a low graze angle, quasi-parallel to the direction of the grooves as shown in Figure 1[1,2]. The light is then diffracted through an arc, forming a cone, so that this mount is also known as conical diffraction. The grating equation in this configuration is

$$\sin\alpha+\sin\beta=\frac{n\lambda}{d\sin\gamma}. \quad (1)$$

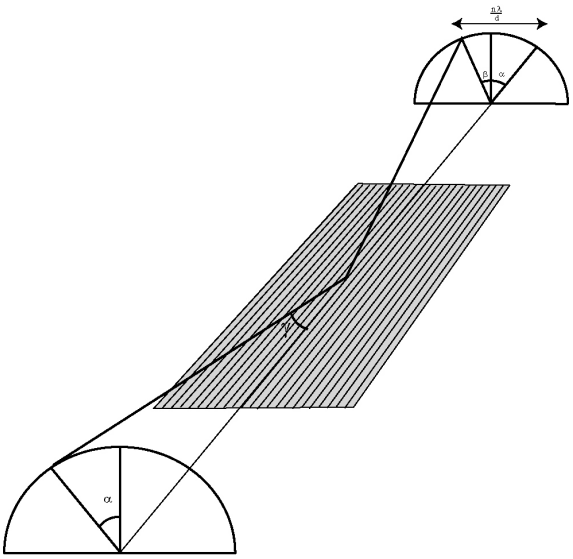

Figure. 1: Geometry of the off-plane mount. Quasi-parallel light at grazing incidence is diffracted in a cone around the direction of the rulings.

where d is the spacing between grooves. γ is the angle between the direction of the incoming ray and the direction of the groove at the point of impact. Light comes into the grating at an azimuthal angle of α along a cone with half-angle γ. It is then diffracted along the same cone of half-angle γ, but now with an azimuthal angle of β.

The off-plane mount supplies the natural geometry for grazing incidence reflection gratings, offering several advantages of which diffraction efficiency and resolution are key. The effective diffraction efficiency of the off-plane mount can be substantially higher than traditional mounts (often a factor of two) due to the groove illumination function[3, 4]. In the off-plane mount the effect of groove shadowing is lessened. Rigorous efficiency calculations of blazed gratings show that the off-plane mount can have efficiencies up to 70% and on average are a few times higher than efficiencies obtainable with a traditional in-plane grating mount[5]. Furthermore, grating imperfections always cause image spreading in the in-plane dimension. Therefore, off-plane resolution is never affected allowing for less sensitivity to grating alignment and grating flatness.

* randy@origins.colorado.edu; phone 1 303 492-5835; fax 1 303 492-5941; http://casa.colorado.edu; Center for Astrophysics and Space Astronomy, Astrophysics Research Laboratory, 593 UCB, 1255 38th Street, Boulder, CO, USA 80309-0593

Optics for EUV, X-Ray, and Gamma-Ray Astronomy, edited by Oberto Citterio, Stephen L. O'Dell, Proceedings of SPIE Vol. 5168 (SPIE, Bellingham, WA 2004)
0277-786X/04/$15 · doi: 10.1117/12.506292

We present here a first-of-its-kind, single pass, grazing incidence, off-plane monochromator for use at X-ray energies.

2. Monochromator

2.1 Fabrication Considerations and Layout

Requirements for the monochromator began with the basic need to provide a monochromatic source of x-rays for off-plane grating testing. Soft x-ray photon energies between 0.2 and 2.0 KeV were required in a moderately collimated and filtered beam. We chose to re-use existing equipment where possible to save on cost and shorten the time-to-service of the instrument. Available equipment included a 0.75" × 3.25" grating with parallel grooves at a density of 4968 grooves/mm and 19 degree blaze angle, a vacuum box, various old UV monochromator parts, and a Manson impact x-ray source. The new monochromator also needed to be positioned in the beam path currently employed by a UV monochromator connected to the large grating test chamber. Approximately 4' of overall length was available in this location, but using this position required that the x-ray instrument be mobile—it must be easily moved back out of the beam path to share time with the UV monochromator.

The X-ray light source is a Manson electron impact source that heats a tungsten filament to create electrons that are accelerated down a voltage gradient to impact a solid anode usually made of carbon, copper or magnesium. Operationally, it was important that the design allow for an expeditious change of the anode without breaking test chamber vacuum and without disturbing the apparatus alignment and/or test configuration. Additionally, it was necessary to maintain a high vacuum (10^{-5} - 10^{-6} Torr, comparable to the grating test chamber) in the vacuum box and in the Manson source. This feature was complicated by the fact that the vacuum box was to be separated from the test chamber by the exit slit and the Manson source separated from the vacuum box by the entrance slit. The Manson source was found to operate unreliably above about 5 x 10^{-5} Torr.

To implement these requirements a grazing incidence geometry was chosen with the incident angle selectable between 0.75 and 2.0 degrees. An off-plane configuration was chosen to allow maximum separation of the orders while maintaining a high throughput. As shown in Figure 2, the grating was mounted in the inside diameter of a manual rotational stage so that it could be rotated to vary the incident/defracted angle (γ in the grating equation) of the beam. A mechanical feed through was employed to rotate the stage, during which the position could be viewed through a Lexan window. A filter holder was positioned downstream of the grating; no allowance was made for the filter to be changed while under vacuum.

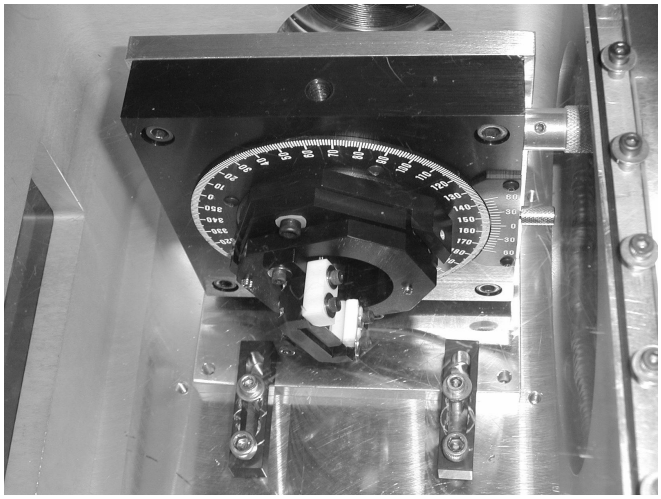

Figure 2: Grating Mount installed on a rotational stage. The mechanical feed through is at the upper right

The overall physical layout can be seen in Figure 3. The following description is provided as a light path sequence. First, the Manson source generates K and L band emission. The photons pass down through a vacuum isolation ball valve and then through the entrance slit about 16" from the source. After the slit, the moderately collimated beam passes through a flexible bellows. This bellows allows the incident beam to be adjusted to varying grazing incidence angles (by changing the selected mounting screw hole pattern for the entrance plate) without affecting the stationary vacuum box. Once inside the vacuum box, the photons strike the grating at grazing incidence in the off-plane configuration. The grating is positioned during alignment (discussed later) to an angle equal to half of the incident beam's offset from the exit beam, placing the cone of diffraction and zero order onto the exit slit. Thus, as the grating is rotated, the cone of diffraction rotates and the higher orders are aligned onto the exit slit one after the other. Both the entrance and exit slits can be adjusted to manipulate the beam to the desired size and intensity. The beam then passes through an aluminum filter during its approximately 16" travel to the exit slit. This filter limits the amount of underlying continuum in the spectrum which increases with increasing X-ray energy. After the exit slit, a second flexible bellows is employed to

couple the monochromator to the grating test chamber. The test chamber is also connected via a flexible line to the vacuum box to allow the chamber's vacuum equipment to maintain the monochromator's volume at the desired high vacuum. This connection can be seen in the lower left portion of the digital photo in Figure 3. The Manson source is evacuated using a separate turbo-molecular pump.

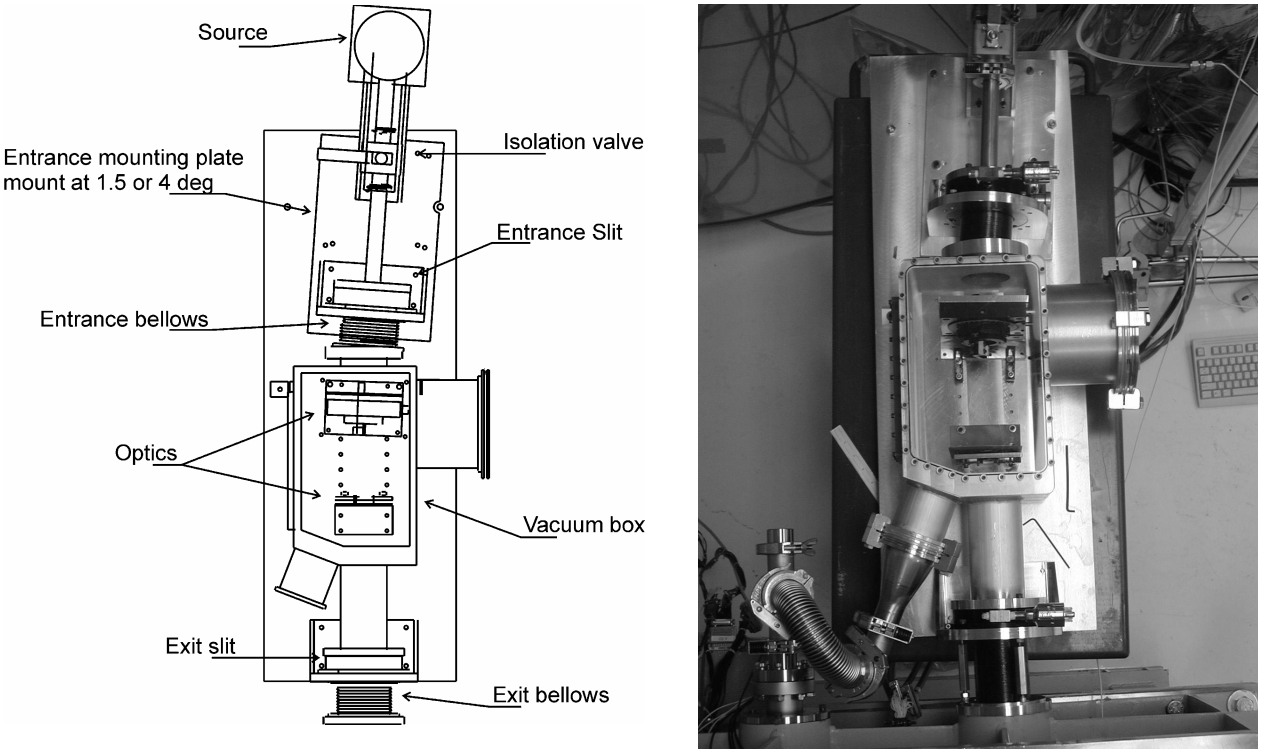

Figure 3: On the left is the complete layout of the X-ray monochromator. On the right is a digital photo of the monochromator as seen from above. It is connected to the grating test vacuum chamber which can just be seen at the bottom of the picture. The Manson source is just off the top edge of the photo.

The instrument was designed locally and commercially fabricated. One significant issue encountered was that the simpler grating mount that was initially employed did not allow for easy adjustment over any of its six degrees of freedom. Therefore, the monochromator required a time-consuming alignment process to prepare it for the most basic grating testing. For subsequent service, a new multi-axis grating mount was developed as seen in Figure 2 that has improved and simplified instrument alignment as discussed in §2.3.

2.2 Vibration Concerns

In order to prevent problems caused by vibration in the optical system, key parts of the monochromator were designed with the highest possible natural frequency so as to decrease the amplitude of any vibrations. One area of vibration affecting the design of all parts was the table on which the instrument was to sit. To maximize the natural frequency of the table, the monochromator was designed to be as light as was practical.

The large base plate (Figure 4) presented another vibration hazard with large unsupported areas between the plate's three leveling feet. Making the plate thicker was not an option because it would add too much weight to the instrument while a stiffer, more complex cross-section would have been too expensive to manufacture. Through analysis of possible vibration modes an acceptable solution was found. The natural frequency of the plate was calculated for several modes, facilitating the selection of a mode with both an acceptably high frequency and a shape that could be

defined with the leveling feet. The i=4, j=1 mode possessed a high frequency and a convenient shape. By mounting the leveling feet along the node lines of this mode, the plate would be able to vibrate in the i=4, j=1 mode while any lower frequency modes would be precluded.

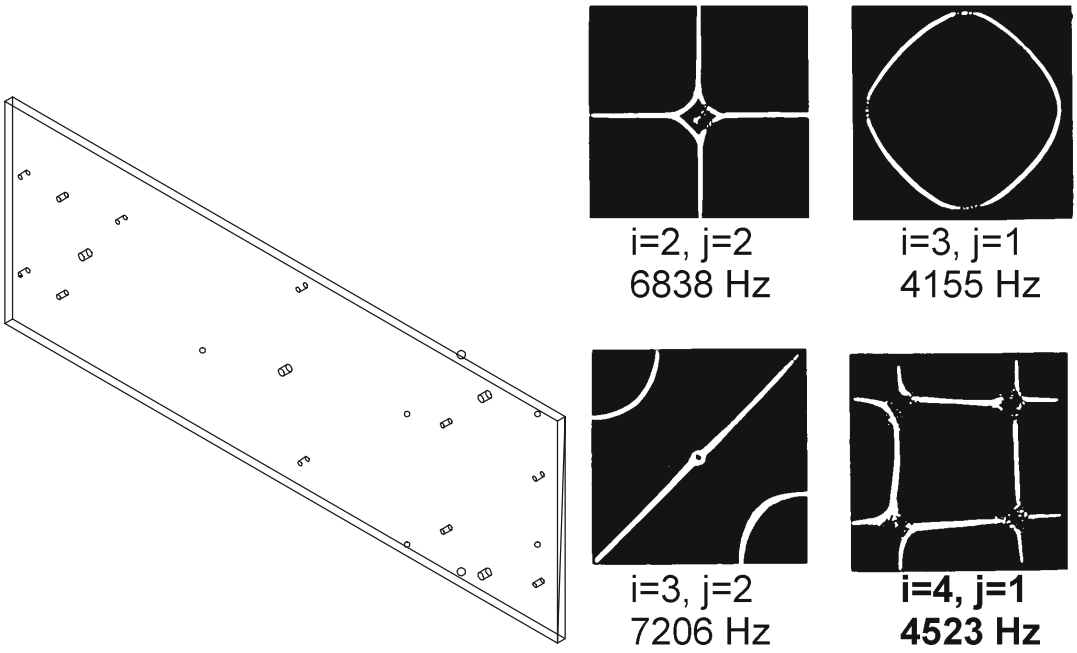

Figure 4: On the left is a CAD drawing of the base plate. On the right are possible vibration modes. The i=4, j=1 mode on the lower right gives convenient node lines along which supports to the plate could be mounted.

The x-ray source used on the monochromator had a large post attached, forcing the source to be cantilevered off the end of the table so that the post could protrude below. A cantilevered mass has the potential to vibrate both vertically and rotationally. These two modes were analyzed for several beam cross-sections and a u-shaped channel determined to be the most stable option (Figure 5).

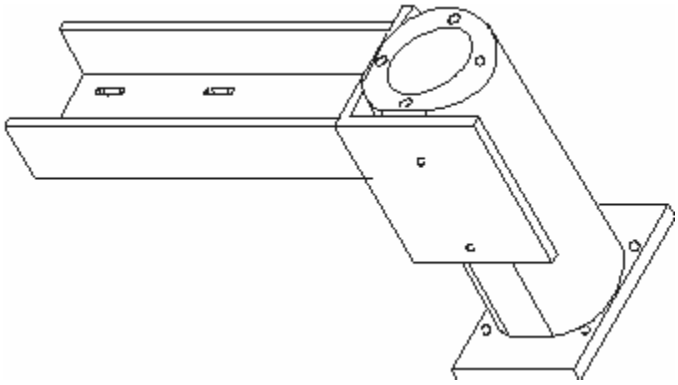

Figure 5: X-ray source mount. The large post that supports the grating is the cylindrical piece on the right. A u-shaped channel was fabricated to mount to the base plate for stability.

2.3 Grating Mount Redesign

Preliminary testing of the monochromator indicated that precise grating alignment would be required if the instrument was to function as designed. Misalignment in grating yaw, pitch and location within the rotational stage led to low count rates, asymmetry in the arc of diffraction as seen through the exit slit, and unidentifiable lines. To facilitate proper alignment, a grating mount was designed with adjustments for translation perpendicular to the grating, yaw and pitch (Figure 6).

The new mount was designed around a full length grating cradle. This cradle supports the entire grating along one precise square edge to fix the orientation of the grating and to limit deformation. Teflon pads on leaf springs hold the grating in place. Grating translation is facilitated by the part labeled “slide”, which is held against the base plate by bolts with elastic washers. Pressing against one end of the slide are compression springs, opposed by a setscrew on the

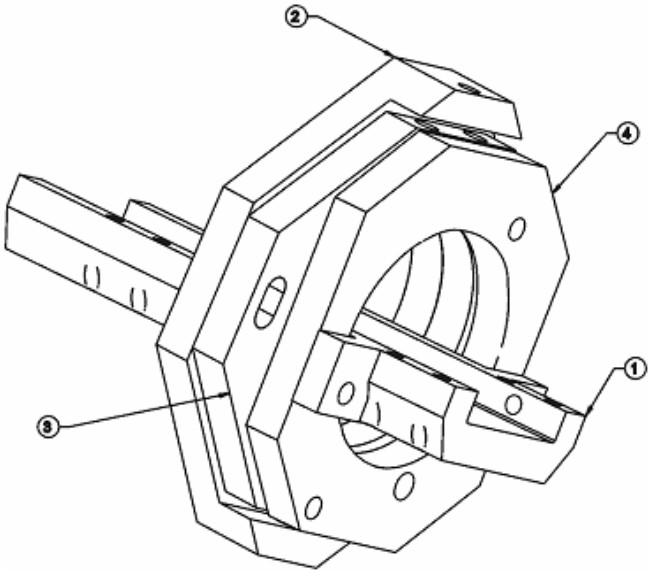

Figure 6: The improved grating mount design where 1 is the cradle, 2 the base plate, 3 the slide and 4 the tip-tilt plate.

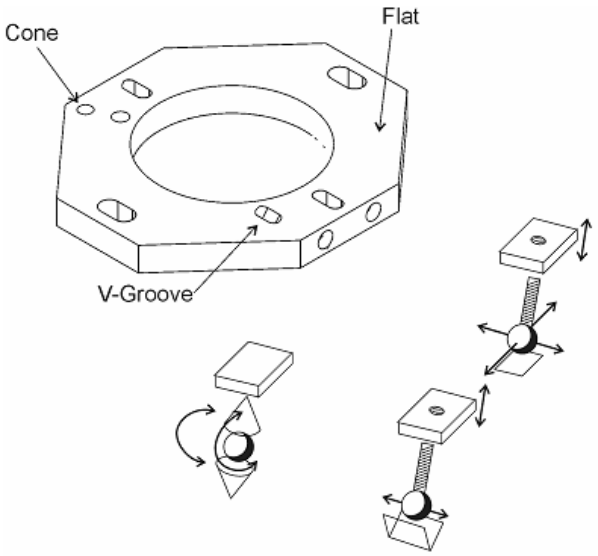

Figure 7: Schematic representing the degrees of freedom contained within the kinematic mount that supports the tip-tilt plate in the grating mount.

other end for adjustment.

The two angular degrees of freedom are provided by the tip-tilt plate, featuring a kinematic mount. This mount supports the tip-tilt plate atop the slide with three mounting points: two sphere tipped setscrews and one ball bearing (Figure 7). Adjusting either setscrew rotates the tip-tilt plate around the ball bearing. The ball bearing is held between conical indentations in either plate to prevent the tip-tilt plate from translating atop the slide. To prevent yaw rotation around the ball, one of the set screws sits in a v-shaped groove. The entire tip-tilt assembly is held to the slide by a stiff compression spring nested over a bolt.

2.4 Alignment

The goals of alignment were to position the grating such that the axis of the rotational stage lay in the plane of the grating, parallel to the groves, and to position the rotational stage at the desired graze angle in such a way that the arc of diffraction would remain centered on the exit slit.

To provide a baseline for alignment and simulate the incident beam, a laser was directed at the entrance slit of the monochromator and autocollimated off of a mirror mounted over the slit. To roughly position the rotational stage, a target printed onto transparency film was centered on the stage, and the stage moved so that the laser passed through the center of the target. The transparent target was then mounted near the monochromator exit slit, centered on the baseline laser. Next, the grating was placed in the instrument and the grating mount adjusted until the reflected laser traced a symmetric arc on the target. Finally, a few adjustments to the position of the rotational stage were needed to center the arc on the exit slit.

2.5 Predicted Behavior

The output of the monochromator can be predicted for any graze angle γ, by solving the grating equation for the dispersion angle β. Below is shown the predicted output in first and second order, for both graze angles and with a few significant energies highlighted.

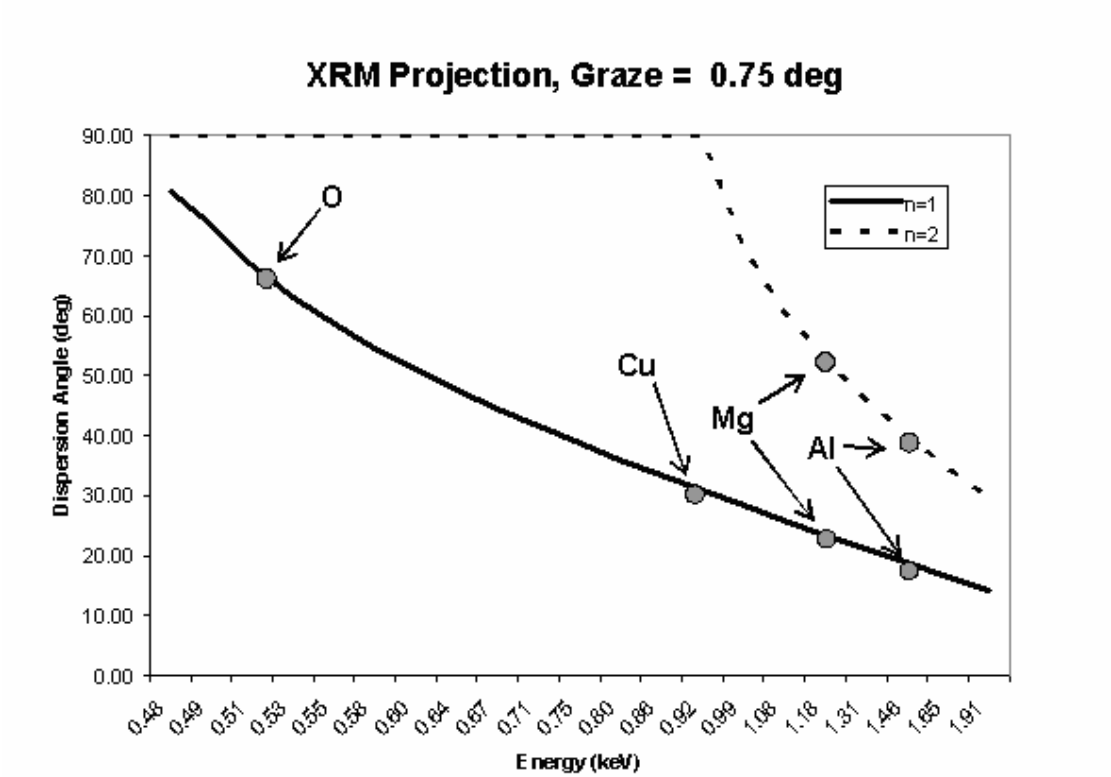

Figure 8: Predicted dispersion angles as a function of energy at first and second order. The energies of relevant lines are labeled. The graze angle on the monochromator grating is 0.75 degrees in this case.

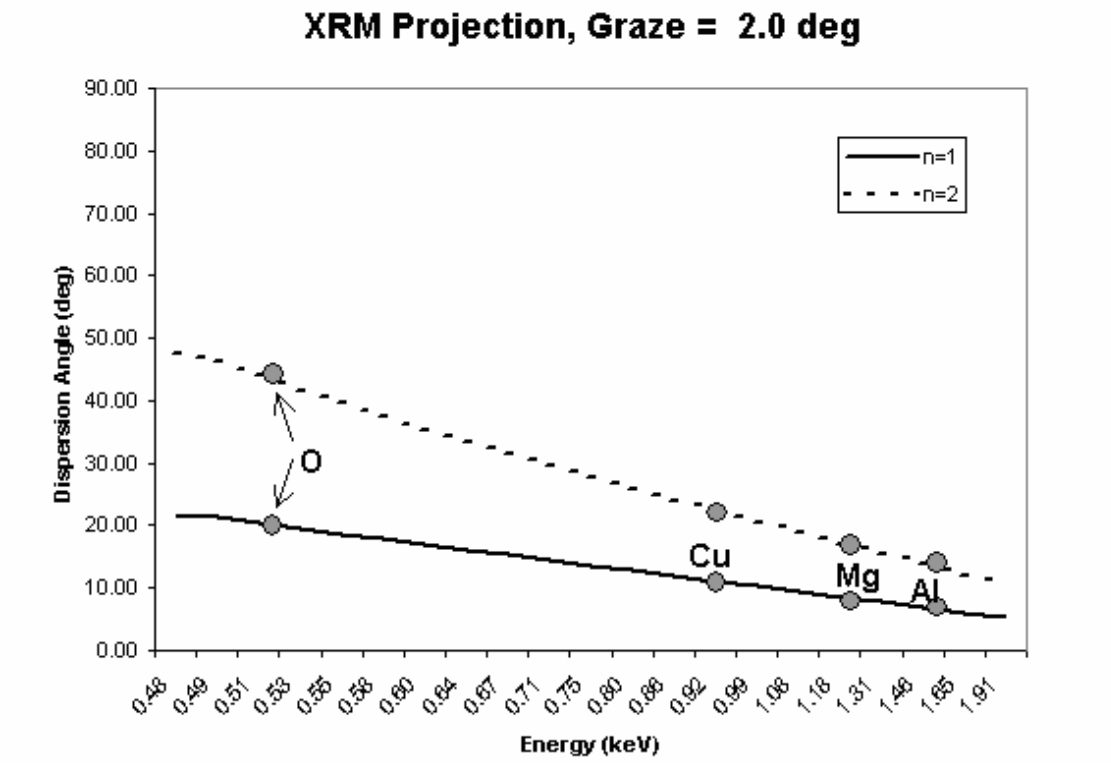

Figure 9: Predicted dispersion angles as a function of energy at first and second order. The energies of relevant lines are labeled. The graze angle on the monochromator grating is 2.0 degrees in this case.

The first graze setting, $\gamma = 0.75$ deg, has the attractive feature of only one available order at energies less than about 1 keV, meaning that no light will be lost to other orders. The same cannot be said of the $\gamma = 2.0$ deg case, but higher orders could not be avoided if lower wavelengths are to disperse out. In this setting, however, the oxygen line at about 0.5 keV, one of the most important lines for our research, lies on the blaze (19 deg). In the $\gamma = 0.75$ deg case, aluminum at about 1.5 keV, another significant line, is on the blaze. The primary disadvantage shown in these early predictions is the impossibility of seeing all of the important spectral lines at one setting. In the $\gamma = 0.75$ deg setting, carbon, around 0.2 keV, has no physical solution and cannot be seen. Also, oxygen appears down towards $\beta = 60$ deg. If the alignment of the grating is not perfect then lines at higher angles, such as oxygen, might not be projected on the exit slit. In the $\gamma = 2.0$ deg setting the higher energy lines of magnesium and aluminum appear at very low angles where they will be difficult to separate from the zero order, un-diffracted light. By adjusting the graze angle γ, one could tune the monochromator to operate in any desired energy region.

2.6 Calibration

All that was needed to calibrate the monochromator was a straightforward comparison between the predicted results and observed spectra. For each spectrum, the output of the monochromator was observed at all positions of the rotational stage and bright areas identified. Throughout testing, observed bright lines (shown as dark regions in Figure 10) on the

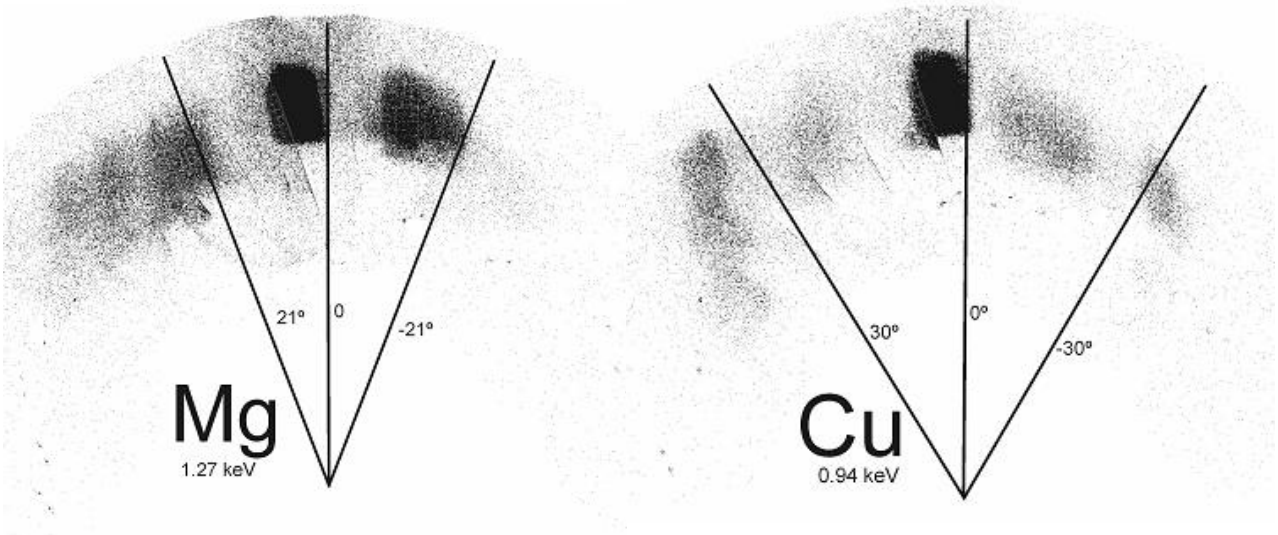

Figure 10: Typical spectra seen off the monochromator. These images are a composite of several detector exposures.

spectrum coincided well with predicted locations, allowing the important features of each spectrum to be unambiguously identified. Figure 10 shows typical spectra, composites from several detector images with lines indicating the predicted spectral line positions. Table 1 lists the locations of the three lines tested.

A common feature seen with all anodes is a significant number of counts surrounding 0 order, extending between ten and twenty degrees on either side. Dispersed light in this area corresponds to photon energies between 1.5 and 2keV. As there should be no sharp emission at this energy and the features are large and blurred, they are probably caused by broadband continuum emitted by the source. This sort of noise in the system is to be expected when running the source at high voltages. For the most part, the monochromator successfully separates this noise from the important signals, although the higher energy lines of magnesium and aluminum come quite close to the continuum. This problem could be solved by closing down the exit slit or using an aperture stop just before the test grating to cut off the nearby continuum at the cost of fewer counts of signal reaching the test grating.

An interesting feature of the composite images is blurred and elongated features at high positive angles. This phenomenon is probably a result of misalignment. When adjusting the monochromator across high angles, prominent features begin to move down and across the detector rather than disappearing off the bottom of the image. As most of

the alignment work was done at settings between +45 and –45 degrees, it is possible that any misalignment out beyond this range escaped our attention.

Anode	Photon Energy (keV)	Predicted Location (deg)	Observed Location (deg)	Photons / second	Source Voltage (keV)
Al	1.51	-18	-17	103	3
	1.51	18	20	103	3
Mg	1.25	-21.5	-20	157	3
	1.25	21.5	22	211	3
Cu	0.94	-30	-30	39	2
	0.94	30	35	92	2

Table 1: Calibration results for the monochromator at three different energies.

3. Results

To confirm that the bright spots we observed were indeed monochromatic, the output of the monochromator was dispersed by a second diffraction grating and these spectra observed. Preliminary results from a high density test grating, also in the off-plane mount, display that this system is a highly effective tool for determining grating efficiencies. In the test setup the monochromatic light enters a vacuum chamber. Within the vacuum chamber is an aperture stop followed by the test grating which diffracts light onto a micro-channel plate detector. The detector is slewed across the focal plane to obtain several exposures which are concatenated together to form the image seen in Figure 11. On the left is the direct beam. On the right is the characteristic arc of dispersion seen with the off-plane mount. The spots are are clean Oxygen-K emission lines at 0.525keV. Nearly all photons are at an energy of 0.525keV because if not the lines would be elongated along the arc of diffraction blurring out the spectral line. Instead, the lack of continuum allows the lines to reproduce the shape of the aperture stop. The production of sharp spectral lines off of the test grating verified the monochromatic nature of the light exiting the monochromator.

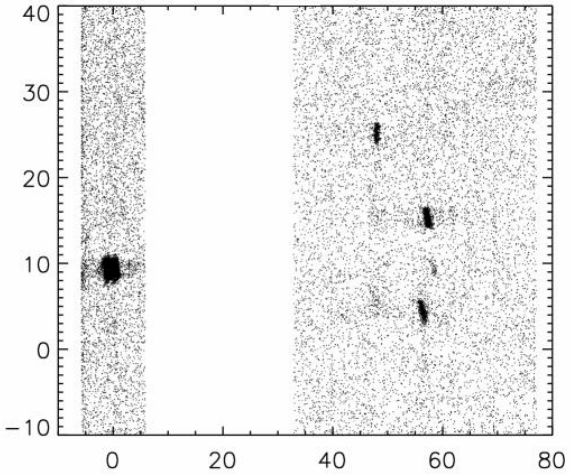

Figure 11: Oxygen-K 0.525keV data of a test grating using clean light from the monochromator

Absolute diffraction efficiencies can now be calculated for the test grating[6]. The background is sampled in the regions of the direct beam and the diffraction arc. Then the number of counts in the direct beam and each of the spectral lines are corrected by this background. Finally, the number of corrected counts in each of the lines is divided by the number of corrected counts in the direct beam to obtain a diffraction efficiency for each of the orders.

4. Conclusions

A novel X-ray monochromator has been developed and constructed. This instrument is used to improve the capabilities of the grating evaluation facility at the University of Colorado in the X-ray regime. The monochromator incorporates a single high groove density grating in the off-plane mount to produce a highly dispersed spectrum from which lines can be chosen to perform evaluations on test gratings. This monochromator was characterized utilizing a variety of source anodes and voltages. The empirical spectra obtained from these characterizations matched theoretical predictions.

Preliminary results from a high density test grating, also in the off-plane mount, display that this system is a highly effective tool for determining grating efficiencies due to the monochromatic nature of the light.

Acknowledgements

We wish to thank Ann Shipley and Mike Kaiser for help with this effort. The work was supported by NASA grant NAG5-11850.

References

1. W. Cash, "X-ray optics. 2: A technique for high resolution", *Applied Optics*, **30**, 1749-1759, 1991.
2. R. Catura, R. Stern, W. Cash, D. Windt, J.L. Culhane, J. Lappington, K. Barnsdale, "X-ray Objective Grating Spectrograph", *Proc. Soc. Photo-Opt. Instr. Eng.*, **830**, 204-216, 1988.
3. M. Neviere, D. Maystre, W.R. Hunter, "On the use of classical and conical diffraction mountings for XUV gratings", *JOSA*, **68**, 1106-1113, 1978.
4. W. Werner, "X-ray efficiencies of blazed gratings in extreme off-plane mountings", *Applied Optics*, **16**, 2078-2080, 1977.
5. L.I. Goray, "Rigorous efficiency calculations for blazed gratings working in in- and off-plane mountings in the 5-50Å wavelength range", *Proc. Soc. Photo-Opt. Instr. Eng*, these proceedings.
6. R.L. McEntaffer, S. Osterman, W. Cash, J. Gilchrist, J. Flamand, B. Touzet, F. Bonnemason, C. Brach, "X-ray performance of gratings in the extreme off-plane mount", *Proc. Soc. Photo-Opt. Instr. Eng*, these proceedings.